CREEP-FATIGUE DAMAGE ANALYSIS ON PR-STRAINED STAINLESS STEEL TYPE321 BY TUBE WORKING IN AN OPERATING BOILER

M. NAKASHIRO*, T. YOSHIDA*, M. KITAGAWA* and H. UMAKI**
*Research Institute and **Electric Power Division
Ishikawajima-Harima Heavy Industries Co., Ltd.
1-15 Toyosu 3-Chome Koto-ku, Tokyo, Japan

ABSTRACT

The power boiler tube (ASTM Type 321) at the bending part failed by creep-fatigue due to start-up and shut-down thermal stresses. For the remaining 111 identical parts, the residual life had to be assessed with damage analysis based on fatigue, creep and creep-fatigue properties investigated on pre-strained material. The damage evaluation method included inspecting the microstructures led to the discovery of small initial fatigue cracks in the samples due to repair work. It can be defined the possibility of failure tube by damage analysis and a few samples inspecting.

KEYWORDS

Pre-strain hardening, Creep, Fatigue, Creep-Fatigue, Stainless steel, Boiler tube, Damage analysis, Residual life assessment

INTRODUCTION

Cautions have been taken in designing the boiler by considering not only the primary stresses due to internal pressure or the self weight, but also the secondary stresses which arise from the unequal temperature distribution that is given rise to on start-up and shut-down or during variable load operations.

An outlet superheater, which is connected to corresponding header stubs of power boiler, has developed a leak. It was made of ASTM TYPE 321 stainless steel(SUS321: JIS), and was cold bent in order to relieve the thermal stresses. The damage was found in the bent part at the inner surface of the tube. In the case of 18-8 type austenitic stainless steels, pre-strain can often cause problems because their work hardening rate is large. In the present case, the effects of pre-strain are reported to be such that the low cycle fatigue strength is not affected or increased somewhat, while the creep strength decreases (Ogawa et al,1986),(Gold et al, 1975),(Moen et al, 1976). This paper discusses the observations made in analyzing the leakage accident mentioned above, pertaining to the nature of the crack, the remaining service life for the undamaged tubes and the creep fatigue properties. An attempt is also made for a practical and simple method for estimating the life of pre-strained SUS321 in the actual service conditions.

BRIEF DESCRIPTION OF THE INCURRED DAMAGE

The leakage took place at the bent of the superheater outlet tube in the #2 in No.2 panel of 111 panels, where the bent radius of #2 tube in each panel was smaller than other 6 member panel

assembly, and a crack developed from its inner side. The total boiler operation time was 58,000h and the cyclic number of start-up and shut-down was 562. Metallographic inspection revealed that the crack was initiated at the outer surface and propagated inwards in the intergranular fracture mode. As the fracture was seen to have propagated into the circumferential direction, the damage was judged to have been induced by creep fatigue due to thermal stress. Inspecting all the #2 tubes of the 111 panels, an other tube also contained a crack, in which opposite to the damaged tube the No.110 panel.

SAMPLE AND METHODS OF TESTING

Several 200mm long pipes were cut out of the sample tube and divided into two groups. One groups was left intact and called the standard, "S" specimen, and the other ones were compressed in their axial direction to 160mm in a press so as to give rise to a compressive strain of 20%, approximately the same as to which the inner side of the failed tube had been bent. These were the pressed, "P" specimen. Figure 1 presents the metallography and hardness of the S and P specimen. While the microstructure is a typical solution treated structure for S specimen, the P specimen revealed a lot of slip lines in the grains and increased hardness from the original Hv144 to Hv263, evidently as a consequence of the applied cold work. Subsequently, test pieces were machined out of these samples.

The creep test was conducted at higher temperatures between 570 and 750℃ with the applied stress varied between 8 and 30kgf/mm^2. The fatigue test was done at 570℃ for a strain range of 0.5, 0.7, or 1.0% with a strain rate of 0.1%/sec. The creep fatigue test was performed also at 570℃ and for a stress holding time of 10 or 60min. with a strain range of 0.7 or 1.0% with a strain rate of 0.05%/s. All specimens were inspected for cracks on completion of the test.

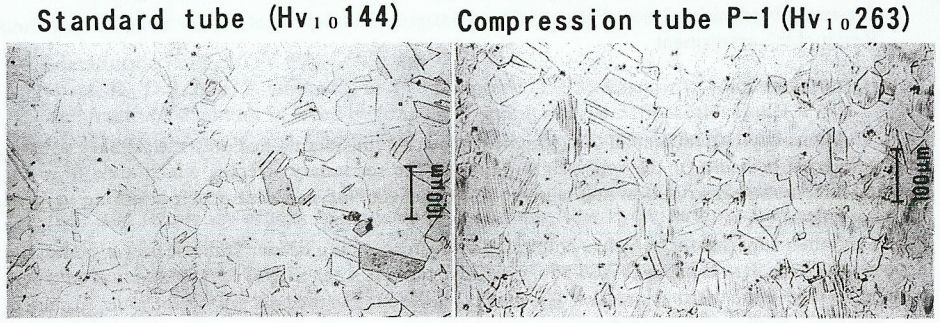

Fig.1 Microstructures of the specimens (S: Standard; P: Pre-compressed).

EXPERIMENTAL RESULTS

(1)CREEP TESTS RESULTS: Figure 2 shows the results of the creep test. The P specimens were all of one half to one tenth in the creep fracture ductility in terms of elongation and reduction in area in comparison to the S specimens. The strength of P specimens was no more than 80 to 90% in stress level of the S specimens, which was in good accord with the average of NRIM Creep Data Sheet(No.5B, 1987).

(2)FATIGUE AND CREEP FATIGUE TEST RESULTS: The results of low cycle fatigue and creep fatigue tests are given in Figure 3. At the same strain amplitude, P specimen plastic deformation is smaller than S. Though the fatigue strength is greater for the P specimen while the strain amplitude is small, the difference becomes smaller with increasing strain amplitude. Figure 4 shows the relations found between the strain and the applied cyclic stress in reference to the monotonic tensile stress and strain curves. It is evident that where the S material works to higher

stress, the P material remains on the monotonic feature curve. Figure 5 shows the variation of stress amplitude with cycles. Where S work hardens with cycles, P remains the same stress amplitude. P has its hardening saturated in the pre-deformation process, so that no further hardening by fatigue is apparent.

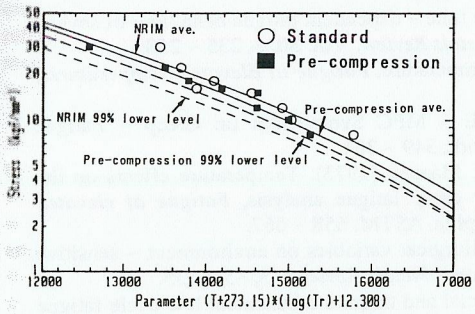

Fig.2 Stress vs Larson-Miller parameter curves and creep data.

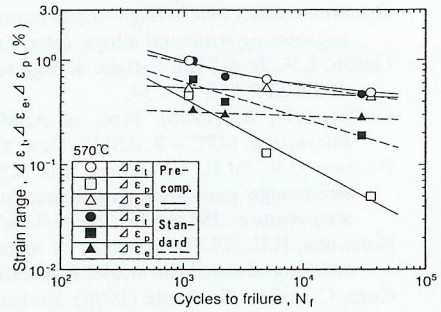

Fig.3 Comparison of fatigue strength between S and P type of specimen.

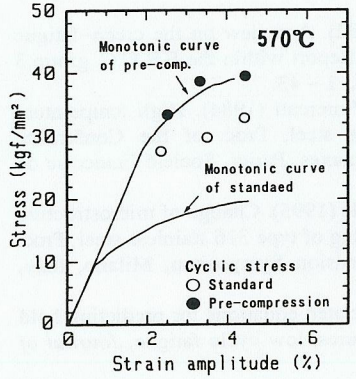

Fig.4 Relationship between strain amplitude and stress to compare with the monotonic tensile stress-strain curves.

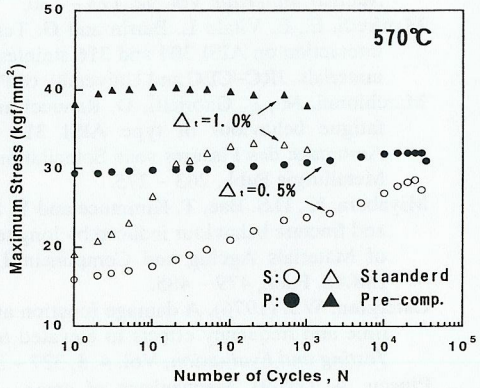

Fig.5 Variation of stress amplitude with cyclic number.

The results of creep fatigue tests showed that the life of P specimen is shortened more than that of S specimen by extending the holding time. This is substantiated by Figure 6, which shows the first cycle of the 60min. hold relaxation curves. Though practically no stress relaxation takes place either in P or in S, the stress level is higher for P than for S, and therefore P with its lower creep strength has its creep fatigue strength degraded much more, hence sustains more damage, than S. Since the application of the linear damage accumulation law has been shown to be the simplest and most effective way to assess the creep fatigue damage, the results were evaluated by linear summation rule and as shown in Figure 7. It will be appreciated that the linearity holds true with a precision of about±25%(Kubo et al, 1993).

In fatigue tests, the fracture mode is transgranular, both in S and in P, but in creep fatigue, it becomes mixture of trans- and inter-granular. The intergranular mode is more prevalent in P than in S, or with the hold time prolonged to give rise to the greater creep damage. The fracture mode in the actual failure appears to be on the extrapolation of this trend.

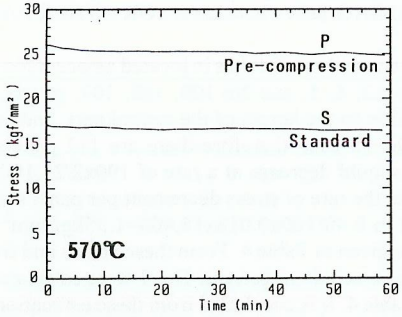

Fig.6 Relaxation curves of creep-fatigue test in 1st cycle.

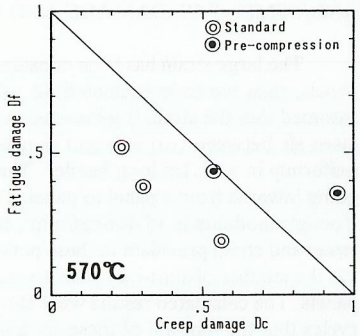

Fig.7 Creep-fatigue damage assessment results by linear summation rule.

STRESS ANALYSIS ON ACTUAL SERVICE CIRCUMSTANCE AND DAMAGE ASSESSMENT

The measured temperature at various points around the outlet header on a start-up showed a differential to be no more than ±3℃, but it was quite large vertically across the header, as shown in Figure 8. The temperature differential can vary from +40℃ to -20℃ during the start-up time. Such a temperature differential naturally brings about distortion in the header, as depicted in Figure 8, it warps first up-wards, then down-wards. Then, this distortion gives rise to progressive changes in stress and strain in the bend part of the outlet superheater tubes as shown schematically in Figure 9. The whole process is an open hysteresis in four steps in which the strain is compressive first, turning to tensile after a while, and finally returning to the state of zero strain when the steady state is reached, but leaving behind a tensile stress, which operates through the rest of the steady state operation of the boiler.

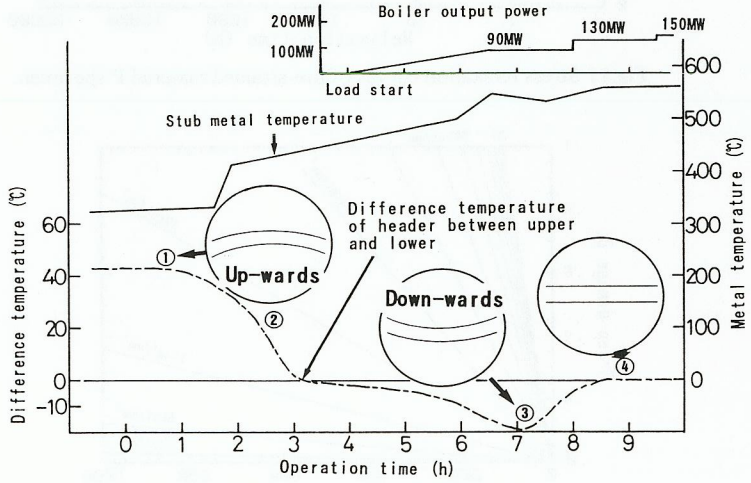

Fig.8 Temperature variation and difference curves of super-heater outlet header during hot start condition.

Elastic analysis was carried out by using mechanical properties listed in Table 1. The calculated results are summarized in Table 2. Subsequently, the hysteresis curves were reconstructed for several different panels based on these strains and the Young's moduli, taking the 0.2% offset strengths as the yield point (Table 1) and assuming no more work hardening takes place once the yield point is exceeded. They are shown in Figure 10 together with the case of S for reference. The stress remaining after a full cycle of hysteresis depends rather sensitively on the magnitude of strain and the yield strength of the material. The results of computation have been summarized in Table 3.

The assessment of creep fatigue damage followed, based on the data shown in Table 3 and the characteristics of creep and fatigue was determined for 570℃, which is the upper limit of service temperature. Figure 11 shows the stress relaxation curves for pre-strained material assuming a steady state creep rate of one tenth. Thus the relaxation exponent was one order of magnitude smaller than that for solution heat treated normal material. For the creep rupture elongation of P specimen was just about one tenth of S specimen. It will be noted that the stress relaxation behaviors shown here correspond quite well to the results obtained by the 60min. holding creep fatigue tests shown in Figure 6. Creep damage evaluation took placed with the mean value of the creep strengths shown in Figure 2 for P. Assuming the temperature changes took place every once in 100h on average similarly as shown in Figure 8 and the number of start-up leading to leakage was 562 and

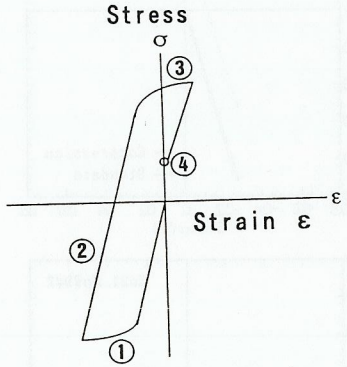

Fig.9 Stress-strain hysteresis loop model at bend region by temperature difference on header between upper and lower position.

Table 1 Mechanical properties of SUS321.

Step No.	Temp. (℃)	Elastic mod. (kgf/mm²)	$\sigma_{0.2}$ (kgf/mm²) S	P
1	300	18, 000	27	46
2	450	16, 900	25	44
3	550	15, 700	23	41
4	570	15, 400	22	39

Table 2 Result of strain evaluation along the hysteresis curve shown in Fig.10.

Step	①	②	③	④
Difference temperature	40℃	0	-20℃	0
Warp of header	4mm	0	2mm	0
No. 2•No. 110 #2	-0. 33%	0	0. 16%	0
No. 2•No. 110 #3	-0. 28%	0	0. 14%	0
No. 1•No. 111 #2	-0. 18%	0	0. 16%	0
No. 1•No. 111 #3	-0. 18%	0	0. 16%	0
No. 21•No. 89 #2, 3	-0. 14%	0	0. 00%	0

Note: Evaluate position is bend region

Table 3 Calculated stress on bend region of tube.

Panel and stub number	Stress, kgf/mm²	$\Delta\varepsilon_1$ %
No. 2, No. 110 #2	14. 0	0. 49
No. 2, No. 110 #3	3. 0	0. 42
No. 21, No. 89 #2	-2. 5	0. 14
*No. 1, No. 111 #3	2. 0	0. 34
*No. 1, No. 111 #3	2. 0	0. 34

Note:*is difference of curvature on another stub.

the operation time was 58,600h, the amounts of damage from the stress relaxation curves of Figure 11 can be calculated. The results are shown in Figure 12, in terms of the accumulated creep damage Dc as plotted in a function of the number of hot start cycles. The fact that this figure indicates Dc to attain unity on about 600th start-up when the applied stress is 14kgf/mm^2 attests to the authenticity of our analytical results shown in Table 3 as represented by the case of #2 tube in No.2 and No.110 panels. Here, it is noted that the creep damage in other parts are negligible, and that simple fatigue damage does not call for serious attention. The actual strain amplitude is small enough to exempt the fatigue strength from design consideration, and, even for a strain amplitude as large as 0.5%, the service life should be more than 10,000 cycles.

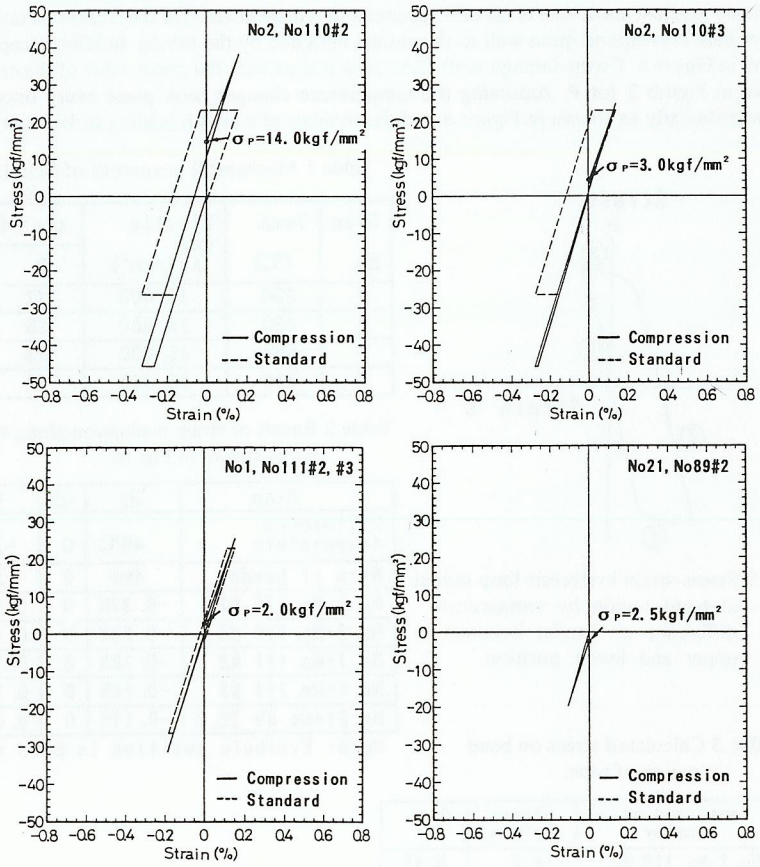

Fig.10 Stress-strain hysteresis loops at bend region for several different tubes by elastic strain analysis results.

ASSESSMENT OF DAMAGE AND REMAINING SERVICE LIFE FOR OTHER PANELS

The large strain has been considered to occurred on #2 tubes in located adjacent No.2 and 110 panels, then we have evaluated #2 tubes in No.3, 4, 5, and No.109, 108, 107, panels. It can be assumed that the strain is generated in proportion to the length of the central part, and because the intervals between two adjacent panels are 190mm each therefore there are 111 panels arranged uniformly in a 21.1m long header. The strain should decrease at a rate of 190x2/21,100=0.018 as going inwards from a panel to panel. Therefore, the rate of stress decrement per panel should, if the Young's modulus is 15,400kgf/mm^2, be equal to 0.49/100x0.018x15,400=1.35kgf/mm^2. Then the stress and strain prevalent in these panels are as given in Table 4. From these values and from Figure 12, the number of start-up cycles to reach at the creep damage value Dc=1 were calculated for each panels. The calculated results were shown in Table 4. It is concluded from these estimation of failure cycles that the renewal of these six tubes should be good enough for sound operation.

These six tubes were take out one year later after the leakage incidence, in which time about 650 times of start-up were carried out. Metallographic examination performed on them revealed that although the No.109 panel tube had early stage microcracks developed as shown in Figure 13,

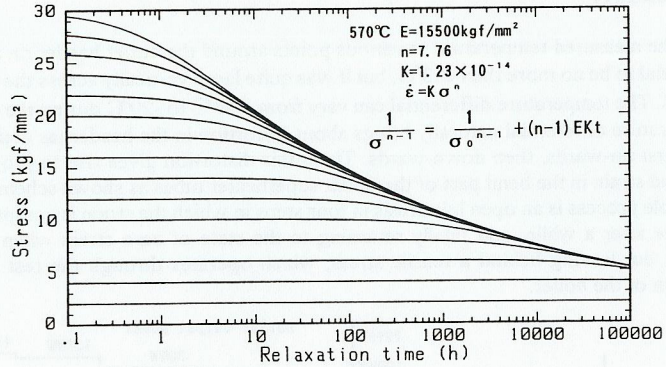

Fig.11 Stress relaxation curves of pre-strained material P specimen.

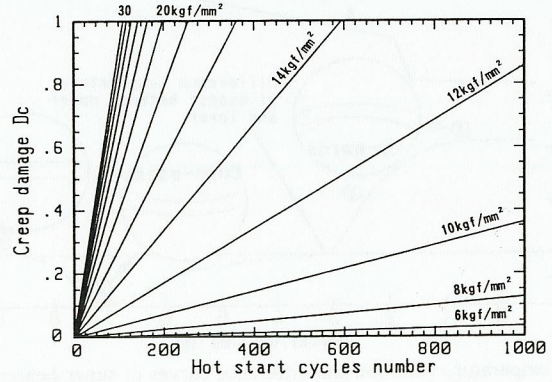

Fig.12 The linear creep damage accumulation characteristics of pre-strained material from calculating the relaxation curves for 100h holding.

other 5 tubes remained undamaged. Therefore, these assessment method were authenticated to be corrected.

CONCLUSIONS

(1)The mechanical properties of pre-strained tubes are somewhat different from normal material. These different properties should be care in applied plants.
(2)The mechanical properties of pre-strained materials should be evaluated by taking the property changes into consideration.
(3)Damage can be evaluated accurately enough on appropriate empirical data and through simplified stress analysis.
(4)Based on the damage assessed, the remaining lives of other apparently undamaged components can be estimated, yet ensuring continuance of operation.

REFERENCES

K.Ogawa, M.Ishi, H.Yoshizawa, B.Ohte, and Y.Wada(1986). Zairyo Vol.35 No.398, pp.56
M.Gold, W.E.Leyda, and R.H.Zeisloft(1975) Trans. ASME305 (Oct.)
R.A.Moen and D.R.Duncan(1976) HEDL-TI-76005
NRIM CREEP DATA SHEET NO.5B (1987)
K.Kubo, S.Kanamaru, and A.Yagi(1983) Zairyo Vol.42 No.427, pp.1

Table 4 Assessment of stress and strain range and estimating results of failure cyclic number for each panel.

Panel No. on #2 stub	Stress kgf/mm²	Strain range %	Cyclic to fail No.
No. 3, 109	12.65	0.48	1000
No. 4, 108	11.30	0.47	1500
No. 5, 107	9.95	0.46	2900

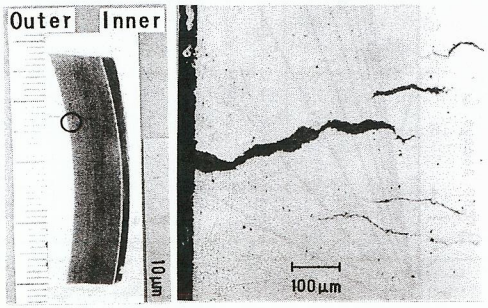

Fig.13 Microcracks formed in the bent of a superheater outlet tube after sampling in about 650 times of hot startups.